J. Anat. (2005) **207**, pp797–811

Atypical development of Sertoli cells and impairment of spermatogenesis in the hypogonadal (*hpg*) mouse

M. Myers,[1] F. J. P. Ebling,[2] M. Nwagwu,[2] R. Boulton,[2] K. Wadhwa,[2] J. Stewart[3] and J. B. Kerr[1]

[1]*Department of Anatomy and Cell Biology, School of Biomedical Sciences, Faculty of Medicine, Nursing and Health Sciences, Monash University, Victoria, Australia*
[2]*School of Biomedical Sciences, University of Nottingham Medical School, Queen's Medical Centre, UK*
[3]*AstraZeneca, Alderley Park, Cheshire, UK*

Abstract

Testes of hypogonadal (*hpg*) mice show arrested postnatal development due to congenital deficiencies of gonadotrophin-releasing hormone (GnRH) and gonadotrophin synthesis and secretion. Follicle-stimulating hormone (FSH), androgen or oestrogen treatment restore qualitatively normal spermatogenesis in *hpg* testes. Understanding the cellular and molecular changes accompanying hormone-induced spermatogenesis in *hpg* mice requires detailed morphological analyses of the germ cells and Sertoli cells in the untreated *hpg* testis. We compared seminiferous epithelial cytology in adult *hpg*, immature and adult wild-type mice using unbiased optical disector-based stereology, immunolocalization of Sertoli cell microtubules (MT), espin (a component of the blood–testis barrier), markers of Sertoli cell maturity ($p27^{kip1}$ and WT-1), and electron microscopy. *Hpg* testes had marked reductions in weight, seminiferous cord volume and length, and severe spermatogenic impairment with germ cells per testis < 1% of adult wild-type testes. Sertoli cell nuclei expressed WT-1 in *hpg* testes, but often were centrally located, similar to 9–14-day-old wild-type testes, and they expressed $p27^{kip1}$, indicating that *hpg* Sertoli cells were post-mitotic. *Hpg* testes had significantly ($P < 0.05$) reduced Sertoli cells per testis (0.56 million) compared with 10-day wild-type (1.15 million) and adult wild-type testes (2.06 million). Immunofluorescence labelling of normal adult Sertoli cells showed supranuclear MT columns and basally located espin, but these features were absent in 10-day-old and *hpg* Sertoli cells. *Hpg* Sertoli cells showed pleomorphic nuclear ultrastructure with mature-type nucleoli, similar to normal adult-type Sertoli cells, but *hpg* Sertoli cells exhibited incomplete tight junctions that lacked ectoplasmic specializations. We conclude that in *hpg* mice, chronic gonadotrophin insufficiency restrains Sertoli cell proliferation and maturation, forming pseudo-adult-type Sertoli cells that are incapable of supporting germ cell proliferation and maturation.

Key words hypogonadal mouse; optical disector; Sertoli cell; spermatogenesis; testis.

Introduction

As first reported by Cattanach et al. (1977a) the hypogonadal (*hpg*) mouse is infertile due to a congenital deficiency of hypothalamic gonadotrophin-releasing hormone (GnRH) synthesis. A deletion in the gene encoding for GnRH results in the inability to produce the mature decapeptide (Mason et al. 1986a,b), leading to a markedly reduced pituitary content of luteinizing hormone (LH) and follicle-stimulating hormone (FSH), and undetectable or barely measurable serum gonadotrophin levels (Cattanach et al. 1977b; Charlton et al. 1983). Consequently, ovaries and testes fail to undergo normal postnatal development (Cattanach et al. 1977a,b). In adult *hpg* males, serum androgen levels are less than 10% of wild-type mice (Singh et al. 1995; Ebling et al. 2000; Haywood et al. 2003), testicular androgen production is barely detectable (Sheffield

Correspondence
Dr Jeff Kerr, Department of Anatomy and Cell Biology, School of Biomedical Sciences, Building 13C, Faculty of Medicine, Nursing and Health Sciences, Monash University, Wellington Road, Clayton, Victoria 3800, Australia. T: (613) 99052723; F: (613) 99052766; E: jeff.kerr@med.monash.edu.au

Accepted for publication *16 August 2005*

& O'Shaughnessy, 1988; Scott et al. 1990) and the number of Leydig cells per testis in adult *hpg* mice is only 10% of normal values (Baker & O'Shaughnessy, 2001). Spermatogenesis in *hpg* testes is arrested at the early primary spermatocyte stage, and coupled with a reduced population of Sertoli cells, the weight of the *hpg* testis in adult mice reaches only 5% that of the age-matched normal testis (Cattanach et al. 1977a; Singh et al. 1995; Ebling et al. 2000). Accurate assessment of cell types and their numbers in the seminiferous epithelium provides important data for interpretation of the physiological regulation of testicular development and the role of endocrine and local growth factors that initiate spermatogenesis.

The *hpg* mouse provides a useful model to study the cell and molecular biology of spermatogenesis in a situation of selective withdrawal of gonadotrophic and androgen hormone support. Importantly, spermatogenesis can be activated in *hpg* testes with exogenous GnRH, androgen, oestrogen or FSH (Charlton et al. 1983; Singh et al. 1995; Handelsman et al. 1999; Ebling et al. 2000; Allan et al. 2001, 2004; Haywood et al. 2003). Although other studies have described the histology of the *hpg* seminiferous epithelium, a detailed evaluation of the Sertoli cells is not available. Quantitative data on individual germ cell types and Sertoli cells are markedly variable depending upon the methods applied to the histological sections (Singh et al. 1995; Handelsman et al. 1999; Baker & O'Shaughnessy, 2001; Haywood et al. 2003). Significant differences in cell quantification values of the *hpg* testicular phenotype raise difficulties in comparing results between laboratories and especially for evaluating control vs. experimental conditions. The proliferation and maturation of Sertoli cells is critical for normal germ cell development in the postnatal testis (Sharpe et al. 2003).

We have examined Sertoli cell maturation in the *hpg* testis using novel, unbiased stereological techniques, electron microscopy and immunolabelling of its cytoskeleton, including those components associated with the inter-Sertoli cell tight junctions. The latter form the blood–testis barrier as the germ cells enter the process of meiotic maturation. We used the expression of the Wilms' tumour transcription factor (WT-1) as an immunocytochemical marker to assess the distribution of Sertoli cells in the *hpg* testis. WT-1 plays an essential role in gonadal development and sexual differentiation (Kreidberg et al. 1993; Luo et al. 1994). It is expressed in fetal Sertoli cells in the mouse, and continues to be expressed at high levels throughout development (Del Rio-Tsonis et al. 1996), thereby providing a stable and robust marker of Sertoli cells. We also investigated the expression of p27 in the *hpg* testes. This cyclin-dependent kinase inhibitor is associated with the inhibition of proliferation in that it disables the cyclin E complexes that initiate the G1/S transition of the cell cycle, and once Sertoli cells pass the G1 restriction point they are committed to completion of the cell cycle (Holsberger et al. 2003). Whereas rather low levels of p27-immunoreactivity are detected in immature Sertoli cells (Millard et al. 1997), intense p27 staining is only found in the nuclei of post-mitotic Sertoli cells (Beumer et al. 1999; Cipriano et al. 2001), thereby providing an index of functional maturation.

The final aim was to quantify the total germ cell population in the *hpg* seminiferous epithelium using the fractionator/optical disector stereological technique (Myers et al. 2004), which is assumption-free with respect to cell size, shape or distribution within the seminiferous epithelium (Wreford, 1995; Wreford et al. 2001). We compared the data (quantitative, ultrastructure and immunolabelling) from the *hpg* mutant with the normal adult and 10-day-old mouse testis, the last of these chosen as it is developmentally immature, a designation assumed to be appropriate to the histological and functional status of the *hpg* testis (Singh et al. 1995; Ebling et al. 2000; Allan et al. 2001). The present study provides baseline information for further quantitative studies exploring the hormonal regulation of Sertoli cells, spermatogonial stem cells and spermatogenesis in the *hpg* testis.

Materials and methods

Animals

All studies were carried out in C3H *hpg* mice from a breeding colony at the School of Biomedical Sciences, University of Nottingham, originally derived from a stock purchased from Jackson ImmunoResearch Laboratories, Inc. (Bar Harbor, ME, USA). Testes from *hpg* adults 170–190 days of age (n = 15) were compared with those from wild-type littermates of *hpg* mice from the same colony: 140–190 days of age (n = 9), 9 days old (n = 3), 10 days old (n = 10) or 14 days old (n = 3). All animal procedures were approved by the University of Nottingham Local Ethical Review Committee and

were carried out in accordance with the Animals Scientific Procedures Act (UK) 1986 (project licence PPL 40/2372).

Tissue collection and processing

For tissues allocated to histological analysis, testes were excised, trimmed of fat and connective tissue, fixed for 24 h in Bouin's fluid, weighed and then processed through graded alcohols into either glycolmethacrylate (acrylic) resin (Technovit 7100, Heraeus Kulzer GmbH, Wehrheim, Germany) or paraffin wax. Testes embedded in glycolmethacrylate were serially sectioned at 20 μm and stained with haematoxylin and eosin. Paraffin-embedded testes from the contralateral side were cut at 5 μm and used for immunofluorescence analysis. Testes used for immunocytochemical studies of $p27^{kip1}$ and WT-1 expression were obtained from mice which had been perfused with 4% paraformaldehyde under terminal sodium pentobarbitone anaesthesia. These tissues were post-fixed in 4% paraformaldehyde (PFA) overnight, then processed via graded alcohols and embedded in paraffin wax. Immunocytochemistry was carried out on tissue sections cut at 5 μm. Testes allocated for epoxy resin embedding were fixed for 4 h in a mixture of 0.1 M sodium-cacodylate-buffered 2.5% glutaraldehyde, 2% formaldehyde and 0.1% picric acid. Following post-fixation in osmium tetroxide, and *en bloc* staining with uranyl acetate, tissues were dehydrated and embedded in an Epon–Araldite mixture. For light microscopy, polymerized blocks were cut at 1 μm and stained with toluidine blue. Ultrathin sections were cut with diamond knives, stained with lead citrate and uranyl acetate, and examined with a JEOL 1200cx electron microscope.

Stereology

All stereological measurements and cell estimations were performed using CAST 2002, Stereological Software (Olympus, Denmark) on an Olympus BX51 microscope equipped with an Autoscan stage (Autoscan Systems Pty Ltd, Melbourne, Australia).

Volumetric analysis of testicular compartments was performed on glycolmethacrylate-embedded testes ($n = 6$) from each of the *hpg*, 10-day and adult wild-type mice. A point-counting system was used to measure volume density V_v of seminiferous tubules, seminiferous epithelium and, if present, tubular lumens. Random slides (three per testis) were chosen and testis sections were traced around using the CAST 2002 stereological software. An 81-point grid was superimposed over each section and viewed using a 20× objective lens with a minimum of ten randomly sampled areas per tissue section. The number of point (P) intersections superimposed on the above components was counted and the volume of the testicular component $V_{v(structure)}$ was obtained by dividing the number of intersection points on each structure by the total number of points i.e.

$$V_{v(structure)} = P_{(structure)}/P_{(total)}.$$

Volume percentage was calculated by multiplying $V_{v(structure)}$ by 100. Volumes of components per testis were determined by multiplying $V_{v(structure)}$ by the whole testicular fixed volume, the latter being numerically equal to fixed testicular weight as the specific gravity of testicular tissue is very close to 1.0.

The diameters of seminiferous tubules were measured across their shortest axis using a measurement function in CAST 2002. Three or four diameters were measured per histological section, and three sections were randomly chosen over six animals per group. Total tubule length (L) per testis was then calculated by the equation

$$L_{(tubule)} = V_v(\text{seminiferous tubule})/\pi r^2$$

where V_v(seminiferous tubule) is the total volume of seminiferous tubules per testis and r is the average radius of the tubule.

A fractionator/optical disector design was used to estimate total germ cell and Sertoli cell numbers in 20-μm stained sections of glycolmethacrylate-embedded adult and 10-day old wild-type, and adult *hpg* testes. Germ cells were identified with the nucleus as a marker, and Sertoli cells were identified by their characteristic shape and/or nucleolar and chromatin morphology as described in the Results section. Germ cells within the seminiferous epithelium were identified according to previous classifications (Oakberg, 1956; Russell et al. 1990; Chiarini-Garcia & Russell, 2001). Cell counts were made using a 100× oil-immersion objective (numerical aperture = 1.4) on an Olympus BX51 microscope equipped with an Autoscan stage. Sections were sampled and germ and Sertoli cell estimates were made using the CAST 2002 stereological system to generate a sampling grid and unbiased counting frames as previously described (Wreford, 1995; Myers et al. 2004).

Immunofluorescence and immunohistochemistry

Immunofluorescence was performed on 5-μm paraffin sections prepared on polylysine-coated microscope slides. Sections were dewaxed, rehydrated and washed in PBS and immersed in 0.01 M citric acid (pH 6.0) for microwave antigen retrieval for 10 min. After cooling to room temperature, sections were then washed in PBS and blocked with 300 mM glycine in PBS for 10 min, 0.1% Triton X in PBS for 10 min and incubated in 10% normal goat serum for 20 min. Primary antibodies diluted in PBS were incubated overnight (β-tubulin 1 : 200, espin 1 : 100 – both primary antibodies kindly supplied by Dr Liza O'Donnell, Prince Henry's Institute of Medical Research, Clayton, Australia). Sections were incubated with Alexa Fluor goat anti-mouse IgG secondary antibodies (fluorophores 488 and 594, Molecular Probes, Eugene, OR, USA) for 1 h. For labelling nucleic acids, sections were incubated in DAPI (Sigma-Aldrich, NSW, Australia) for 15 min, washed in PBS and mounted with fluorescence mounting medium (DAKO, NSW, Australia).

Immunoperoxidase histochemistry was carried out on 5-μm paraffin sections that were initially prepared as above. After the antigen retrieval procedure, sections were incubated for 5 min in 3% hydrogen peroxide to quench endogenous peroxidase activity, washed in PBS and incubated in 1.5% normal goat serum for 30 min. Sections were incubated with the primary antibodies overnight: p27 mouse monoclonal antibody (NCL-p27) was obtained from Novocastra Laboratories (Newcastle, UK) and used at a working dilution of 1 : 25. WT-1 rabbit polyclonal antiserum (sc-192) was obtained from Santa Cruz Biotechnology Inc (Santa Cruz, CA, USA) and used at a working dilution of 1 : 200. Both primary antisera were diluted in PBS containing 1% Tween 20 and 0.3% bovine serum albumin (both Sigma, Poole, UK). On day 2, sections were washed in PBS and incubated in biotinylated secondary antisera as appropriate (Vector Laboratories, Peterborough, UK), then washed and incubated with an avidin–biotin–horseradish peroxidase complex as per the manufacturer's instructions (Vectastain Elite kit, Vector Laboratories). Immunoreactivity was revealed by incubation in a solution of diaminobenzidine (Sigma), after which sections were counterstained with eosin, dehydrated and mounted in DePeX (Sigma).

Statistical analysis

Statistical analysis was performed using SigmaStat 3.0 (Jandel Scientific, San Rafael, CA, USA). Data for each group of mice were compared using a one-way ANOVA in conjunction with Tukey's *post-hoc* test. All data are presented as mean ± SEM, and the level of significance at $P < 0.05$ is indicated.

Results

General testis morphology

A quantitative assessment of testicular components is presented in Table 1. Testis weight in *hpg* mice was less than half that of 10-day-old mice and only 3% of adult wild-type testes. Development of seminiferous cords in *hpg* testes was markedly impaired in comparison with normal adults, with cord or tubule diameter, total volume per testis and cord or tubule length significantly ($P < 0.05$) smaller. Hypogonadal testes contained less than 1% of the total germ cell population of adult wild-type testes (0.5 vs. 66.3 million per testis, respectively).

Histology

The seminiferous epithelium of the adult wild-type testis showed cell and tissue architecture expected of full spermatogenic activity (Fig. 1A). Germ cells of all types were arranged as a complex stratified epithelium. The Sertoli cells showed typical mature morphology, notably large basally located nuclei with a prominent nucleolus

Table 1 Quantitative assessment of testicular components in adult and 10 day wild-type and adult *hpg* mouse testes

	Adult	10 day	*hpg*
n	6	6–7	6–9
Body weight (g)	28.5 ± 2^a	6.5 ± 0.3^b	27.5 ± 3^a
Testis weight (mg)	77.0 ± 8^a	5.3 ± 0.4^b	2.3 ± 0.2^b
Tubule or cord diameter (μm)	222.0 ± 4^a	79.0 ± 1^b	68.0 ± 2^c
Tubule or cord volume (μL)	72.0 ± 7^a	5.0 ± 0.3^b	2.0 ± 0.2^b
Seminiferous epithelium volume (μL)	65.0 ± 7^a	5.0 ± 0.3^b	2.0 ± 0.2^b
Total germ cells/testis (10^6)	66.3 ± 4^a	2.2 ± 0.8^b	0.5 ± 0.1^b
Tubule length (m)	2.0 ± 0.2^a	1.0 ± 0.1^b	0.6 ± 0.1^b

^{a,b,c} represent whether a significant difference ($P < 0.05$) was observed between different groups.

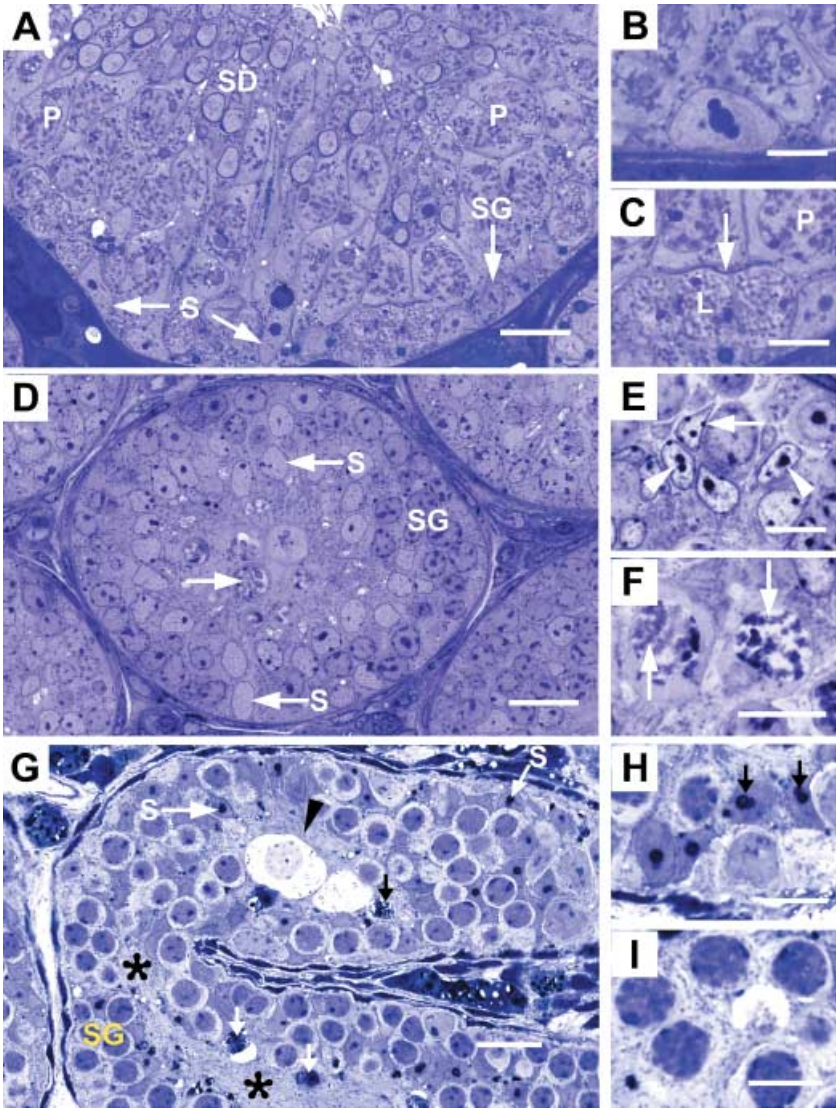

Fig. 1 Histology of seminiferous epithelium in adult wild-type (A–C), 10-day-old wild-type (D–F) and adult *hpg* testis (G–I). (A) Adult wild-type seminiferous epithelium at stage IX of spermatogenic cycle showing nuclei of Sertoli cells (S), spermatogonium (SG), pachytene primary spermatocytes (P) and early elongating spermatids (SD). (B) Detail of a mature Sertoli cell nucleus with a tripartite nucleolus. (C) High-magnification of A showing leptotene (L) and pachytene (P) primary spermatocytes between which is a thin curvilinear structure (arrow) representing inter-Sertoli cell junctional complex. (D) Ten-day wild-type testis showing basal and central Sertoli cell nuclei (S), spermatogonia (SG) and occasional spermatocytes (arrow). (E) Detail of Sertoli cell nuclei showing ovoid and angular shapes with small nucleoli (arrowheads) and heterochromatin patches (arrows). (F) Most advanced germ cell type is occasional primary spermatocytes showing condensed chromatin (arrows). (G) *hpg* testis cord showing basal and central Sertoli cell nuclei (S), spermatogonia (SG) and central confluence of Sertoli cell cytoplasm (asterisks). Degenerative cellular debris (arrows) and hydropic-type germ cells are indicated (arrowhead). (H) Detail of Sertoli cell nuclei showing large and double-nucleoli (arrows). (I) Most advanced germ cells are zygotene primary spermatocytes with thickened chromatin profiles. Scale bars in A, D, G, = 20 μm; all others = 10 μm.

that in favourable sections is tripartite in structure (Fig. 1B). In the basal region of Sertoli cell cytoplasm, thin densely stained curvilinear structures were noted (Fig. 1C). These represent segments of the inter-Sertoli cell tight junctions that partition the seminiferous epithelium into basal and adluminal compartments, the so-called 'blood–testis' barrier.

In the 10-day wild-type testis the seminiferous cords were typically immature, their diameter being only one-third of tubules in the adult (79 vs. 222 μm, respectively). The seminiferous epithelium occupied the whole of the cord as no lumen was present (Fig. 1D). Although the extent of spermatogenic activity was variable between individual tubule sections, the most advanced germ cells were zygotene or (uncommonly) pachytene primary spermatocytes (Fig. 1F). The Sertoli cells showed a relatively consistent morphology. Their nuclei were ovoid or angular, occasionally located close to the basal lamina but more often displaced centrally within the cords. Nucleoli consisting of a single clump of chromatin were noted, together with small patches of heterochromatin associated with the nuclear membrane (Fig. 1E). These features are characteristic of the immature Sertoli cell. The central regions of cords were occupied by confluent regions of Sertoli cell cytoplasm. Linear or curvilinear structures corresponding to inter-Sertoli cell junctions were not observed.

Seminiferous cords of the *hpg* testis were smaller in diameter compared with the 10-day testis (68 vs. 79 μm, respectively) and showed considerable curvature, as evidenced by a mixture of longitudinal (Fig. 1G) and cross-sections. Spermatogenesis had advanced to the zygotene (and rarely pachytene) primary spermatocyte stage (Fig. 1I). Products of cell degeneration and hydropic-type

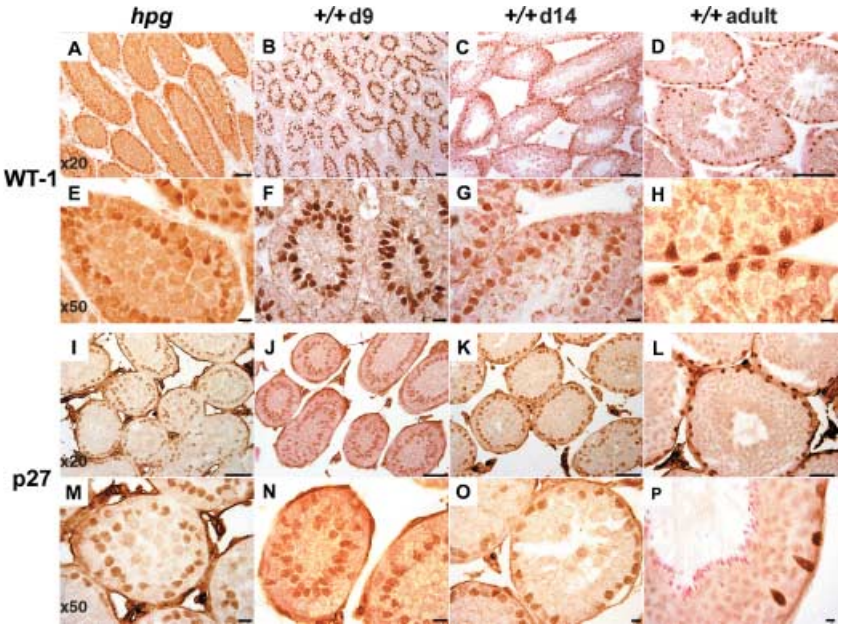

Fig. 2 Expression of WT-1 (upper panels) and p27 (lower panels) immunoreactivity in adult *hpg* mouse testis (far left column: *hpg*) or wild-type mouse testes on postnatal day 9 (second left column: +/+d9), day 14 (second to right column: +/+d14) or adult (far right column: +/+adult). For each antigen, the upper row are micrographs obtained with a ×20 objective (scale bars = 30 μm), the lower row obtained with a ×50 objective (scale bars = 10 μm).

germ cells were a common occurrence (Fig. 1G). The Sertoli cells showed unusual morphology. Their nuclei, often crowded together, were located close to the basal lamina and also displaced more centrally, the spermatogonia intervening between them and the peritubular tissue (Fig. 1H). Sertoli cell nuclei showed irregular shapes ranging from ovoid to angular. The nucleoli were prominent, occurring singly or in pairs, and showing double or tripartite morphology and occasional annular nucleoli (not shown at light microscope level). Structures representing the inter-Sertoli cell junctions were not observed.

WT-1 and p27 immunohistochemistry

There was specific immunolabelling of Sertoli cell nuclei with both antisera at all postnatal ages studied and in testes from adult *hpg* mice (Fig. 2). No immunoreactive nuclei were detected in control studies where the primary antisera were omitted (data not shown). A proportion of interstitial cells also had immunopositive staining nuclei using the p27 antiserum, but not using the WT-1 antiserum (Fig. 2). Whereas the intensity of the WT-1 immunoreactivity was similarly high at all ages studied and in the *hpg* testis (Fig. 2A–H), the intensity of the p27 immunoreactivity was generally greater in the adult wild-type testis than in the *hpg* testes or the day 9 and 14 wild-type testes (Fig. 2I–P). WT-1- and p27-immunopositive Sertoli cell nuclei from wild-type testes studied on postnatal day 9 typically had an ovoid or elliptical appearance, and were not in contact with the basal lamina. The lumen has not begun to develop at this age, and the WT-1- or p27-immunopositive cells were not distributed in a single uniform layer (Fig. 2B,F,J,N). By postnatal day 14, a lumen was observable in a proportion of tubules, and the WT-1 and p27 immunoreactivity revealed that in some tubules the Sertoli cells had a more basal location and had become a monolayer (Fig. 2C,G,K,O). In all adult wild-type tubules, the WT-1/p27-immunoreactive nuclei were in close proximity to the basal lamina, forming a single layer, and the nuclei frequently had a characteristic angular appearance (Fig. 2D,H,L,P). The appearance and distribution of WT-1/p27-immunoreactive Sertoli cell nuclei in the *hpg* testes was similar to that of the wild-type testis on postnatal day 9, although some aspects resembled the day 14 testis. In most cords the Sertoli cell nuclei were located centrally relative to the basal lamina, and not clearly stratified into a single layer, but in other cords the nuclei had formed a single layer located closer to the basal lamina (Fig. 2A,E,I,M). A number of nuclei had an angular appearance rather than the ovoid shape more common in testes from postnatal day 9 mice (Fig. 2E).

Immunofluorescence expression of microtubules and espin

In adult wild-type seminiferous tubules, tubulin was strongly localized to the body and the adluminal extensions of the Sertoli cell cytoplasm (Fig. 3A), matching the abundance of microtubules known to occur in the Sertoli

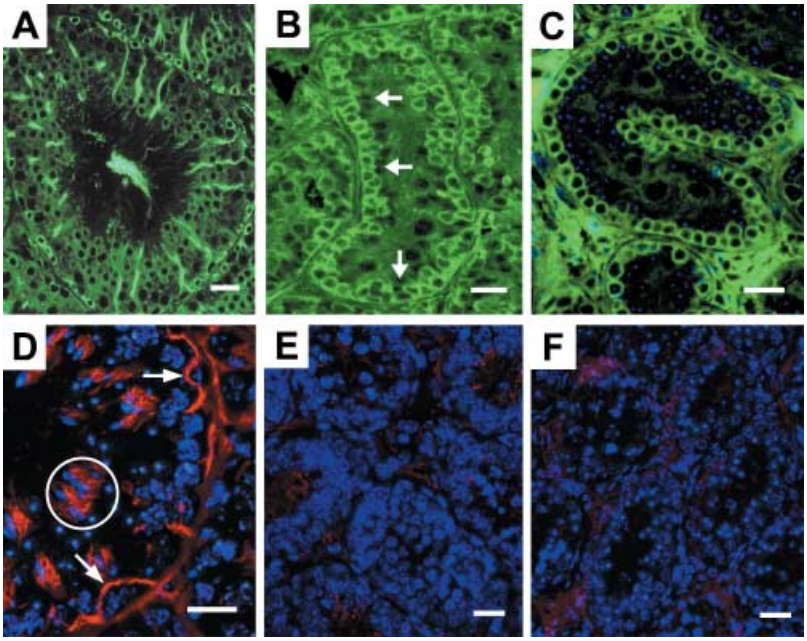

Fig. 3 Immunofluorescence demonstration of microtubules (β-tubulin) indicated by green fluorescence and espin (red fluorescence). Nucleic acids are shown by blue fluorescence. A,D are adult wild-type testes; B,E are 10-day wild-type testes, and C,F are *hpg* testes. (A) Normal adult seminiferous tubule showing tall columns of microtubules in Sertoli cells and surrounding the basal spermatogonia with circular cell nuclei. (B) Ten-day seminiferous cord showing positive tubulin label among circular/irregularly shaped basal cells and weak labelling more centrally where negative profiles of immature Sertoli cells are noted (arrows). (C) *hpg* testis showing positive tubulin label of circular, basal germ cells and absence of tubulin in the centre of the cord. Nucleic acids (blue fluorescence) label more centrally located cells, the identity of which cannot be confirmed. (D) Normal adult testis showing arching and curvilinear segments of the espin component of inter-Sertoli cell tight junctions (arrows). Espin in ectoplasmic specializations of spermatid bundles is indicated (circle). Nucleic acids in nuclei of spermatocytes and spermatids are shown by blue fluorescence. (E) Ten-day testis showing lack of or very weak labelling for espin; blue fluorescence indicates nucleic acids. (F) *hpg* testis showing lack of positive label for espin in the seminiferous cords; blue fluorescence indicates germ and Sertoli cell nuclei. Scale bars, 20 μm.

cell. Positive immunofluorescence was also noted in the cytoplasm of basally located germ cells, forming numerous ring-type profiles. More centrally placed primary spermatocytes and round spermatids did not show significant labelling for tubulin. Tubulin was localized also to basal germ cells in the 10-day wild-type testis (Fig. 3B). Immature Sertoli cells, the nuclei of which could be seen as negative-type images immediately central to the germ cells, showed weak labelling in their central cytoplasmic extensions. In *hpg* seminiferous cords, tubulin was labelled in the cytoplasm of basal germ cells (Fig. 3C). Negative images of the Sertoli cell nuclei containing DAPI-positive nucleoli could be seen but the cytoplasm associated with them and extending into the central region of the cords was not positively labelled for tubulin.

Junctional specializations

The localization of espin, indicating the presence of this actin-binding/bundling protein with the inter-Sertoli cell junctions, was readily observed in the adult wild-type testis. Espin label was seen as curvilinear and arching structures in the basal aspect of the seminiferous epithelium (Fig. 3D), representing the specialized tight junctions. In addition, positive label for espin was observed among clusters of elongating spermatids that are embedded in the columns of Sertoli cell cytoplasm. Here the spermatid acrosomes are closely associated with Sertoli cell ectoplasmic specializations that contain espin. Within the seminiferous cords of the 10-day wild-type testis and the *hpg* testis, espin labelling was absent or very weak compared with the intensity of the label seen in the adult wild-type testis (Fig. 3E,F).

Ultrastructure of Sertoli cells

In adult wild-type testes the Sertoli cell nuclei were located at the base of the seminiferous epithelium and showed pleomorphic shapes ranging from irregularly ovoid (Fig. 4A) to pyramidal. Heterochromatin was

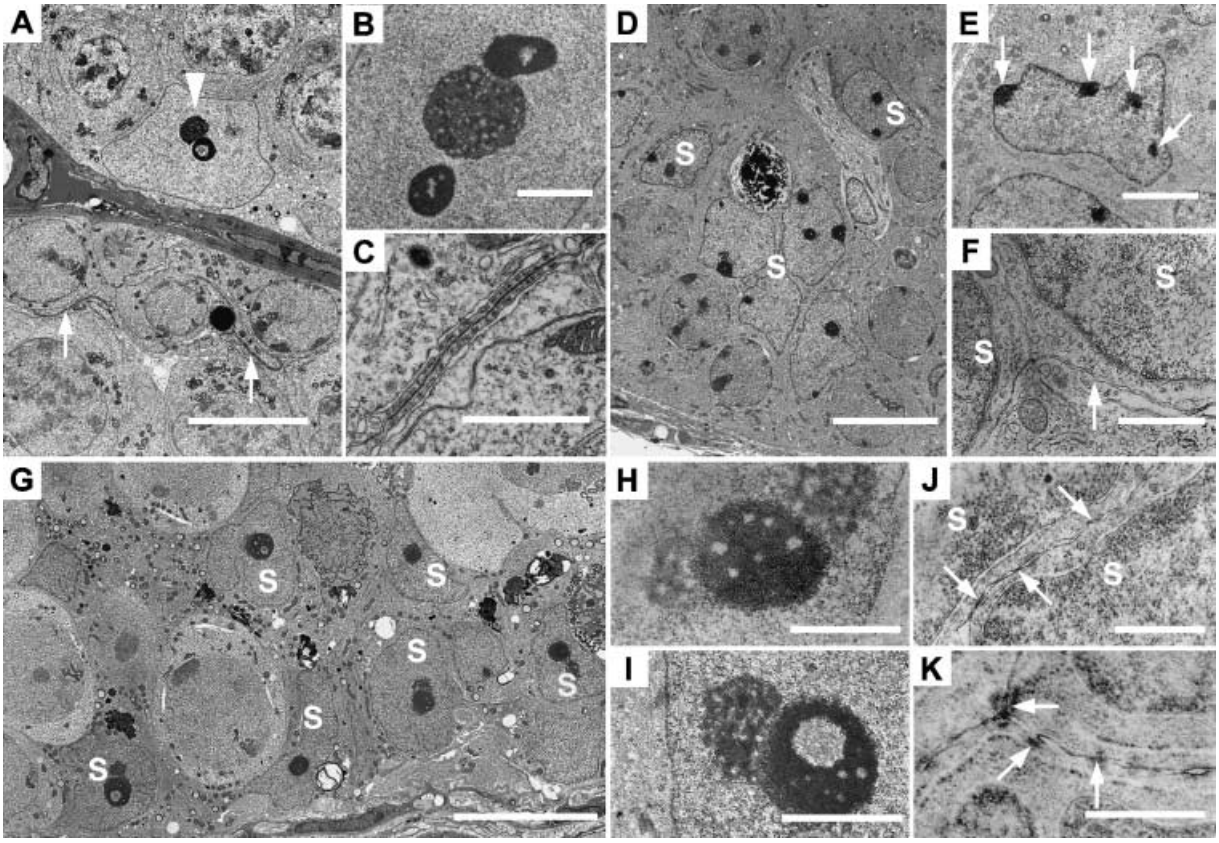

Fig. 4 Electron micrographs of adult wild-type (A–C), 10-day wild-type (D–F) and adult *hpg* testes (G–K). (A) Typical normal adult Sertoli cell with nucleolus and annular chromatin (arrowhead) and curved inter-Sertoli cell junctions (arrows). (B) Sertoli cell tripartite nucleolar complex showing central nucleolus and flanking chromatin. (C) Inter-Sertoli cell junctional complex between apposing Sertoli cells. (D) Ten-day testis with compacted immature Sertoli cell nuclei (S). (E) Immature Sertoli cell nucleus with patches of heterochromatin associated with nuclear membrane (arrows). (F) Unspecialized plasma membranes (arrow) between adjacent Sertoli cell nuclei (S). (G) *hpg* testis showing basal and more central Sertoli cell nuclei (S). (H) Sertoli cell tripartite nucleolar complex with central chromatin and peripheral nucleoli. (I) *hpg* Sertoli cell nucleolar complex showing granular nucleolus and annular chromatin. (J) Plasma membranes between hpg Sertoli cell nuclei (S) showing segments of close apposition of membrane. (K) Plasma membranes between adjacent *hpg* Sertoli cells showing individual cytoplasmic densities. Scale bars in A,D,G = 10 μm; E = 3 μm; B,I = 2 μm; C,F,H = 1 μm; J,K = 0.5 μm.

rarely noted within the nucleus except in association with the nucleolus where one or two heterochromatic masses flanked the nucleolus forming a tripartite structure typical of adult mouse Sertoli cells (Fig. 4B). In some views the chromatin itself showed an annular morphology. Where the plasma membranes of adjacent Sertoli cells became apposed, inter-Sertoli cell junctions were found, at times extending for 10 μm in the basal aspect of the seminiferous epithelium (Fig. 4A). At high magnification inter-Sertoli cell junctions showed the typical morphology of ectoplasmic specializations with subplasmalemmal bundles of actin filaments and membranous cisternae orientated parallel to the apposed plasma membranes of the Sertoli cells (Fig. 4C).

Sertoli cell nuclei in 10-day old wild-type mice were arranged at random within the peripheral aspect of the seminiferous cords, some being proximal to the basal lamina and others being more central (Fig. 4D). These nuclei showed elliptical or polygonal shapes and, depending on the plane of thin section, exhibited one or more small nucleoli together with several clumps of heterochromatin associated with the nuclear membrane (Fig. 4E). The plasma membranes of adjacent Sertoli cells did not show the presence of inter-Sertoli cell junctions (Fig. 4F).

In *hpg* testes the Sertoli cell nuclei exhibited unique morphology with highly irregular shapes due to significant folding and indentation of the nuclear membrane (Fig. 4G). Sertoli cells were found adjacent to the basal lamina and also more centrally where two or more Sertoli cells were stratified. A characteristic feature of *hpg* Sertoli cells was the single, double or tripartite

Table 2 Stereological estimates of cell numbers in adult and 10-day wild-type and adult *hpg* mouse testes. Values are millions per testis and represent means ± SEM

	Adult	10-day	*hpg*
n	6	6–7	7
Sertoli cells	2.06 ± 0.13[a]	1.15 ± 0.08[b]	0.56 ± 0.02[c]
Sp/gonia & preleptotene sp./cytes	2.93 ± 0.32[a]	1.94 ± 0.08[b]	0.31 ± 0.03[c]
Primary sp./cytes	9.40 ± 0.65[a]	0.28 ± 0.03[b]	0.17 ± 0.04[b]
Leptotene to diplotene			
Round spermatids	25.60 ± 1.79	ND	ND
Elongating spermatids	28.47 ± 1.95	ND	ND

ND, germ cell types were not detected.
Superscript letters indicate whether a significant difference ($P < 0.05$) was observed between different groups.

nucleolar complex (Fig. 4H,I) with the chromatin often showing an annular morphology. The plasma membranes of adjacent regions of *hpg* Sertoli cell cytoplasm occasionally showed points of apparent fusion or adherens-type sites of membrane apposition (Fig. 4J). Electron-dense material associated with the apposed Sertoli cell membranes was noted although no clear resolution into particles or filaments was found (Fig. 4K). These regions suggested the rudimentary formation of ectoplasmic specializations but typical fully formed inter-Sertoli cell junctional complexes were not observed.

Cell quantification

Stereological assessments of cell numbers per testis are given in Table 2. Adult wild-type testes had significantly ($P < 0.05$) greater numbers of Sertoli cells compared with 10-day wild-type testes, consistent with the expansion of the Sertoli cell population up to 3 weeks postnatally. In *hpg* testes Sertoli cell numbers showed a 73% reduction compared with adult wild-type testes and were only half of the numbers measured in the 10-day old testes. Similarly, germ cell numbers in *hpg* testes were markedly reduced in comparison with adult testes. Spermatogonia/preleptotene primary spermatocytes per *hpg* testis showed a 90% reduction and primary spermatocytes (leptotene and beyond) showed a 98% reduction compared with the adult wild-type testis. The same classes of germ cells were, respectively, reduced by 84% and by 40% in comparison with 10-day old wild-type testes. No spermatids were noted in the seminiferous cords of 10-day wild-type or *hpg* testes.

To check the reliability of the estimated numbers of germ cells of the *hpg* testes obtained by stereological analysis, we determined the conversion ratios of germ cell classes as they progressed through spermatogenesis in the adult wild-type testis (Table 3). The observed vs. expected ratios between the proliferation and/or maturation of (i) spermatogonia into primary spermatocytes, (ii) primary spermatocytes into early spermatids and (iii) early spermatids into elongating spermatids were similar. These findings confirmed that the individual quantitative data for each class of germ cells were a reliable estimate for the normal adult testis and by inference for the 10-day old wild-type and *hpg* testis, as the same stereological methods were used.

Table 3 Conversion ratios of germ cell types (×106 per testis) in adult wild-type testes

Germ cells	Ratios	Measured	Theoretical
ES 9–16: RS 1–8 =	28.4 : 25.6	1.1	1
RS 1–8: Pach + Dip =	25.6 : 7.4†	3.5	4
Lep-Dip Spc: Spg/Prl Spc =	9.4 : 2.9	3.2	4*

*Based on estimated spermatogonial divisions from Kluin et al. (1984), de Rooij & Grootegoed (1998) and de Rooij & Russell (2000).
ES 9–16 = elongating spermatids in stages IX–XVI of spermiogenesis; RS 1–8 = round spermatids in stages I–VIII of spermiogenesis; Pach + Dip = pachytene and diplotene primary spermatocytes; Lep-Dip Spc = leptotene to diplotene spermatocytes; Spg/Prl Spc = spermatogonia and preleptotene spermatocytes.
†Excludes leptotene primary spermatocytes, which = 1.94.

Estimates of the numbers of germ cells associated on average with a single Sertoli cell were calculated from the primary quantitative values, and are given in Table 4. The data show that on average a single Sertoli cell of adult wild-type testes supports more than 30 germ cells. In 10-day-old wild-type and in *hpg* testes

Table 4 Germ cell load expressed per single Sertoli cell. Values are millions per testis and represent means ± SEM

	Adult	10-day	*hpg*
Sertoli cells per testis (10^6)	2.06	1.15	0.56
Spermatogonia	1.4	1.6	0.5
Spermatocytes	4.5	0.3	0.3
Round spermatids	12.4	ND	ND
Elongating spermatids	13.8	ND	ND
Total germ cells/Sertoli cell	32	2	1

ND, germ cell types were not detected.

the Sertoli cells are associated with far fewer germ cells, the former with two germ cells on average per Sertoli cell and in the latter the ratio is nearly 1 : 1.

Discussion

The hereditary hypogonadism in the *hpg* mouse is an important animal model for idiopathic hypogonadotrophic hypogonadism (IHH) in the human. Although the *hpg* mouse testis appears to phenocopy the human IHH testis, the common characteristics of failure of testicular development and infertility arise from different genetic backgrounds. The *hpg* model results from a 33.5-kb deletion truncating the GnRH gene (Mason et al. 1986a,b), whereas in IHH patients gene mutations/deletions of the GnRH gene itself have not been described (Burns & Matzuk, 2002). In human IHH disorders, gene mutations may disrupt migration of GnRH-releasing neurons (in Kallman's syndrome), impair GnRH processing or prevent the secretion of GnRH, as in studies describing mutations of the GPR54 receptor (Franco et al. 1991; Jackson et al. 1997; de Roux et al. 2003; Seminara et al. 2003). The cytology of the *hpg* mutant mouse testis reported in this study is similar to the brief qualitative histology of the testis recently described in the GnRH receptor (*Gnrhr*) mutant male mouse (Pask et al. 2005), which is another animal model for human IHH involving the GnRHR mutation (Beranova et al. 2001). We have used novel and assumption-free stereological methods to define the cytological status of the seminiferous epithelium of the *hpg* mouse testis in comparison with the normal adult and 10-day-old testis, the last of these chosen as its maturational status is similar to *hpg* with regard to qualitative spermatogenic development. The impairment of testis growth in adult *hpg* mice is seen in testis weight, which was only 3% that of adult wild-type mice, 50% of the weight of 10-day-old wild-type testes, and in total seminiferous cord volume and length per testis, which was 3 and 30%, respectively, in comparison with adult testes. The data show that hypogonadism arising from a congenital deficiency in gonadotrophin secretion is a result of a marked reduction in both the Sertoli cell and the germ cell populations when compared with either the prepubertal (10-day-old) or adult wild-type testis. Severe impairment of spermatogenesis in *hpg* mice is evident because the testis had only 23 and 1%, respectively, of the total germ cell population in comparison with 10-day-old and adult wild-type testes.

The fractionator/optical disector stereological technique is an efficient and unbiased method for estimating total cell numbers per organ. The method is independent of testis volume and the shape, size and distribution of cells within the seminiferous epithelium (Wreford, 1995), and it has been applied to testicular tissue of normal and mutant mice (Robertson et al. 1999, 2002; Kumar et al. 2001; Wreford et al. 2001), rat (Meachem et al. 1998, 1999), monkey (O'Donnell et al. 2001) and human (Zhengwei et al. 1998; Bendsen et al. 2003; Raleigh et al. 2004).

In *hpg* testes, the number of spermatogonia/preleptotene spermatocytes (0.31 ± 0.03 million per testis) was only 10% of their numbers found in adult wild-type testes (2.93 ± 0.32 million per testis). In other studies (Singh et al. 1995; Singh & Handelsman, 1996a,b; Spaliviero et al. 2004) a similar low proportion was reported (8–10%), although the absolute numbers of spermatogonia ranged from 0.12 to 0.6 million per testis in *hpg* mice and from 1.6 to 6.7 million per testis in adult wild-type mice. Spermatogenesis in *hpg* testes advanced no further than zygotene or rarely early pachytene primary spermatocytes, and total spermatocytes were estimated at 0.17 ± 0.04 million per testis, representing only 2% of all primary spermatocytes found in adult wild-type testes (9.40 ± 0.65 million per testis). Although spermiogenesis in the *hpg* mouse was not observed in the present study nor in any of those above, our estimates of round spermatids (25 million per testis) and elongating spermatids (28 million per testis) in adult wild-type mice are similar to those of the C57BL/6 mouse strain (Wreford et al. 2001), where application of the optical disector stereological analysis reported 30 and 27 million per testis for round and elongating spermatids, respectively. We found that the germ-cell-carrying capacity of *hpg* Sertoli cells was

0.7 germ cells per Sertoli cell, in agreement with ratios of 0.7–1.1 that we calculated from the individual cell graphical data reported by other studies (Haywood et al. 2003; Allan et al. 2004; Spaliviero et al. 2004). In adult wild-type testes, the germ cell load per Sertoli cell was 32 germ cells per Sertoli cell, in agreement with ratios of 26–30 that we calculated from other individual quantitative cell data (Robertson et al. 2002; Spaliviero et al. 2004).

The severe hypospermatogenic status of the *hpg* vs. adult wild-type testis affecting both the supply and the maturation of spermatogonia was further emphasized in comparison with the 10-day wild-type testis. At this time occasional pachytene spermatocytes are the most advanced germ cell type noted, but most primary spermatocytes were at the leptotene–zygotene step. The *hpg* testis has only 16% of the spermatogonia/preleptotene spermatocytes present in the 10-day wild-type testis (0.31 ± 0.03 vs. 1.94 ± 0.08 million per testis) and only 60% of the primary spermatocytes (0.17 ± 0.04 vs. 0.28 ± 0.03 million per testis). The low proportion of spermatogonia reflects impaired proliferation among spermatogonial cell types in the *hpg* testis. The higher proportion of primary spermatocytes in the *hpg* vs. 10-day testis is attributable to their maturation arrest and persistence in the 170–190-day *hpg* testis, and the relatively low numbers of primary spermatocytes in the 10-day testis (Wang et al. 1998; Hosoi et al. 2002).

Deprived of endocrine support due to insufficiency of gonadotrophins and testosterone, the cytological response of the *hpg* seminiferous epithelium is expressed not only by impairment of germ cell development but also by alterations in the morphology and number of Sertoli cells. The *hpg* testis contained only 27% of the Sertoli cells found in the adult wild-type testis (0.56 vs. 2.06 million per testis, respectively) and less than 50% of the Sertoli cells counted in the 10-day wild-type testis (1.15 million per testis). Clearly the lack of gonadotrophic support, in particular FSH, results in the failure of Sertoli cells in *hpg* testes to attain their full proliferative and developmental potential. The key and selective role of FSH in stimulating Sertoli cell proliferation is noted in transgenic *hpg* mice expressing FSH. In these mice there is a dose-dependent effect on testis growth in which increasing serum levels of FSH are capable of increasing *hpg* Sertoli cell numbers to wild-type levels (Allan et al. 2004). That FSH is the primary Sertoli cell mitogen in the postnatal *hpg* testis has been emphasized in other studies where neither hCG (human chorionic gonadotrophin) nor testosterone supplementation are capable of stimulating Sertoli cell proliferation to attain the numbers seen in the wild-type testis (Handelsman et al. 1999; Haywood et al. 2003; Spaliviero et al. 2004). In the opposite situation of loss-of-function of FSH using knock-out mice that lack FSH (FSHβKO) or FSH receptors (FSHRKO), Sertoli cell number per testis is normal at birth and in the early postnatal period, but they cease proliferation at 3 weeks and their number remains at about 60% of the wild-type population (Wreford et al. 2001; Johnston et al. 2004).

In previous studies of Sertoli cell histology in *hpg* testes they have been described as exhibiting an immature morphology, i.e. polygonal nucleus lacking or containing a single round nucleolus, the nucleus often centrally located in the seminiferous cord and no apical cytoplasmic extensions (Singh et al. 1995; Singh & Handelsman, 1996a,b; Allan et al. 2001, 2004; Haywood et al. 2002, 2003). These characteristics apply to some but certainly not all *hpg* Sertoli cells that can be identified in histological sections or after immunostaining for WT-1 or p27. Many Sertoli cells in the *hpg* testis show morphological features shared with mature Sertoli cells in the adult wild-type testis, e.g. folded and pleomorphic nuclei, one or more prominent nucleoli, associated heterochromatin forming a paired or tripartite complex, and a basal nuclear location. The expression of p27 immunoreactivity indicates that the Sertoli cells in the *hpg* testis are at least as mature as those in the postnatal day 9 testis, but given the inherently non-quantitative nature of immunoperoxidase histochemistry it is not possible to equate the intensity of the staining to a precise developmental age. Our ultrastructural observations are the first to show that *hpg* Sertoli cells represent a hybrid or transitional morphology between immaturity and full development. Although *hpg* Sertoli cell nuclei show some adult-type characteristics, e.g. tripartite and annular nucleolar development normally found only in mature Sertoli cells (Flickinger, 1967; Kierszenbaum, 1974; Mirre & Knibiehler, 1982), cytoplasmic development is limited, lacking an organized columnar cytoplasm and the occurrence of rudimentary inter-Sertoli cell junctional complexes. The cytoplasm of mature Sertoli cells extends apically through the seminiferous epithelium and provides a central column, with lateral branches, for structural and functional support of the germ cells. The integrity of Sertoli cell cytoplasm in the normal adult testis is dependent upon its cytoskeleton, particularly the rich supply of

microtubule bundles (Vogl et al. 1993) that were readily demonstrated by fluorescence immunocytochemistry. By contrast, microtubules in the *hpg* seminiferous cords were confined to a position circumscribing the Sertoli cell nuclei and the adjacent germ cells but no extensions into the central region of the cords. A similar arrangement of immunolabelled microtubules was observed in the seminiferous cords of the 10-day-old wild-type testis. The lack of cytoplasmic maturity and organization of the cytoskeleton was confirmed by ultrastructural analysis. An additional indicator of Sertoli cell immaturity in the *hpg* testis was the absence of the organelles and cytoskeletal elements (membranous cisternae, actin filament complexes, tight junctions) that together form the intratubular blood–testis barrier between neighbouring mature Sertoli cells. The presence or absence of the barrier among Sertoli cells of *hpg*, 10-day-old and adult wild-type testes was demonstrated by immunolocalization of espin and by electron microscopy. Espin is an actin-binding/bundling protein associated with Sertoli cell–spermatids and Sertoli cell–Sertoli cell ectoplasmic specializations (ES) (Bartles et al. 1996; Chen et al. 1999), the latter found along apposing Sertoli cell plasma membranes forming unique junctional complexes known as the blood–testis barrier (Moroi et al. 1998; Toyama et al. 2003). Identical in structure and position to dense curviform profiles noted by light microscopy, immunolocalization of the espin component of adult Sertoli cell junctional complexes was shown with fluorescence microscopy. Ultrastructural observations of adult Sertoli cells confirmed the expected morphological features of the ES. In 10-day-old testes, specific labeling for espin was not found and junctional specializations were not formed as indicated by electron microscopy. A similar lack of espin labelling and absence of fully organized Sertoli cell junctional complexes was found in *hpg* Sertoli cells, indicating the immature state of *hpg* Sertoli cells. Incompletely formed Sertoli cell junctional complexes in the 12–14-day-old mouse (Byers et al. 1991) and in the diethylstilbestrol-treated mouse testis (Hosoi et al. 2002) do not form an intact blood–testis barrier and both resemble the dysmorphic junctional complexes of *hpg* Sertoli cells. Initiation of spermatogenesis in the normal postnatal testis is associated with the progressive proliferation and maturation of the Sertoli cells and from postnatal day 10–17 the ES are formed and recruited to sites that become the fully developed junctional complexes of the blood–testis barrier (deKretser & Kerr, 1994; Hosoi et al. 2002). Disruption (Wiebe et al. 2000). Delay (Vitale et al. 1973; Toyama et al. 2003) or failure of development (Cavicchia & Sacerdote, 1991; Morales & Cavicchia, 2002; Noguchi et al. 2002) of competent Sertoli cell junctional complexes in the rodent testis is accompanied by impairment of primary spermatocyte maturation, emphasizing the significance of the blood–testis barrier for the early phases of spermatogenesis. The impermeability of junctional complexes (an index of epithelial barrier function) is, however, not an absolute requirement for maturation of spermatocytes but is correlated with development of Sertoli cells, their apical secretion of fluid and the appearance of the tubule lumen (Pelletier, 1986; Setchell et al. 1988; Russell et al. 1989).

Although the *hpg* mouse testis is a model analogous to congenital hypogonadotrophic hypogonadism in men, it does not exactly phenocopy acquired IHH or the variable cytology of Sertoli cells associated with arrested germ cell development in idiopathic hypospermatogenesis. In the latter cases, impaired germ cell development usually at the early mid-primary spermatocyte stage often coexists with Sertoli cells showing histological, ultrastructural or immunocytochemical features that classify them as immature or adult-type or dedifferentiated (Steger et al. 1999; Maymon et al. 2002). Severe impairment of spermatogenesis in the *hpg* testis is accompanied by a low supply of partially mature Sertoli cells that show some adult characteristics but fail to form a structurally organized blood–testis barrier. The incomplete proliferation and maturation of *hpg* Sertoli cells and arrested spermatogenesis 6 months after birth is attributable to chronic insufficiency of gonadotrophic hormones, notably FSH, and intratesticular testosterone content (O'Shaughnessy & Sheffield, 1990; Singh & Handelsman, 1996a). FSH has been shown to exert major stimulatory actions on Sertoli cell and early germ cell development in the *hpg* mouse (Haywood et al. 2003; Allan et al. 2004).

In summary, we have used unbiased stereological analysis of cell types and numbers, immunolocalization of nuclear and cytoskeletal proteins of Sertoli cells, and electron microscopy to study the seminiferous epithelium of the *hpg*, immature and adult wild-type mouse testis. We propose that during postnatal life the seminiferous epithelium of the *hpg* testis shows a cytological response commensurate with a 'drip-feed' exposure to gonadotrophic and androgenic hormones. Sustained low-level hormone stimulation of the *hpg*

testis is sufficient only to support limited Sertoli cell maturation and maintenance of a residual supply of germ cells, as indicated by stereological analysis. Because the *hpg* testis remains responsive to FSH, hCG, androgen or oestrogen, it provides an important animal model for further studies of the molecular mechanisms controlling testicular maturation and spermatogenesis.

Acknowledgements

We thank Dr Liza O'Donnell and Amanda Beardsley for β-tubulin and espin antibodies, Dr Ric Duckett for stereological advice, and Sue Connell, Ian Boundy and Shaun Fleming for technical assistance. This work was supported by an AstraZeneca Collaborative Grant.

References

Allan CM, Haywood M, Swaraj S, et al. (2001) A novel transgenic model to characterize the specific effects of follicle-stimulating hormone on gonadal physiology in the absence of luteinizing hormone actions. *Endocrinology* **142**, 2213–2220.

Allan CM, Garcia A, Spaliviero J, et al. (2004) Complete Sertoli cell proliferation induced by follicle-stimulating hormone (FSH) independently of luteinizing hormone activity: evidence from genetic models of isolated FSH action. *Endocrinology* **145**, 1587–1593.

Baker PJ, O'Shaughnessy PJ (2001) Role of gonadotrophins in regulating numbers of Leydig and Sertoli cells during fetal and postnatal development in mice. *Reproduction* **122**, 227–234.

Bartles JR, Wierda A, Zheng L (1996) Identification and characterization of espin, an actin-binding protein localized to the F-actin-rich junctional plaques of Sertoli cell ectoplasmic specializations. *J Cell Sci* **109**, 1229–1239.

Bendsen E, Byskov AG, Laursen SB, Larsen HP, Andersen CY, Westergaard LG (2003) Number of germ cells and somatic cells in human fetal testes during the first weeks after sex differentiation. *Hum Reprod* **18**, 13–18.

Beranova M, Oliveira LM, Bedecarrats GY, et al. (2001) Prevalence, phenotypic spectrum, and modes of inheritance of gonadotrophin-releasing hormone receptor mutations in idiopathic hypogonadotrophic hypogonadism. *J Clin Endocrinol Metab* **86**, 1580–1588.

Beumer TL, Kiyokawa H, Roepers-Gajadien HL, et al. (1999) Regulatory role of p27kip1 in the mouse and human testis. *Endocrinology* **140**, 1834–1840.

Burns KH, Matzuk MM (2002) Minireview: genetic models for the study of gonadotropin actions. *Endocrinology* **143**, 2823–2835.

Byers S, Graham R, Dai HN, Hoxter B (1991) Development of Sertoli cell junctional specializations and the distribution of the tight-junction-associated protein ZO-1 in the mouse testis. *Am J Anat* **191**, 35–47.

Cattanach BM, Iddon CA, Charlton HM, Chiappa SA, Fink G (1977a) Gonadotrophin-releasing hormone deficiency in a mutant mouse with hypogonadism. *Nature* **269**, 338–340.

Cattanach BM, Murray I, Tracey JM (1977b) Translocation yield from the immature mouse testis and the nature of spermatogonial stem cell heterogeneity. *Mutat Res* **44**, 105–117.

Cavicchia JC, Sacerdote FL (1991) Correlation between blood–testis barrier development and onset of the first spermatogenic wave in normal and in busulfan-treated rats: a lanthanum and freeze-fracture study. *Anat Rec* **230**, 361–368.

Charlton HM, Halpin DM, Iddon C, et al. (1983) The effects of daily administration of single and multiple injections of gonadotropin-releasing hormone on pituitary and gonadal function in the hypogonadal (hpg) mouse. *Endocrinology* **113**, 535–544.

Chen B, Li A, Wang D, Wang M, Zheng L, Bartles JR (1999) Espin contains an additional actin-binding site in its N terminus and is a major actin-bundling protein of the Sertoli cell-spermatid ectoplasmic specialization junctional plaque. *Mol Biol Cell* **10**, 4327–4339.

Chiarini-Garcia H, Russell LD (2001) High-resolution light microscopic characterization of mouse spermatogonia. *Biol Reprod* **65**, 1170–1178.

Cipriano SC, Chen L, Burns KH, Koff A, Matzuk MM (2001) Inhibin and p27 interact to regulate gonadal tumorigenesis. *Mol Endocrinol* **15**, 985–996.

Del Rio-Tsonis K, Covarrubias L, Kent J, Hastie ND, Tsonis PA (1996) Regulation of the Wilm's tumor gene during spermatogenesis. *Dev Dynamics* **207**, 372–381.

Ebling FJ, Brooks AN, Cronin AS, Ford H, Kerr JB (2000) Estrogenic induction of spermatogenesis in the hypogonadal mouse. *Endocrinology* **141**, 2861–2869.

Flickinger CJ (1967) The postnatal development of the Sertoli cells of the mouse. *Z Zellforsch* **78**, 92–113.

Franco B, Guioli S, Pragliola A, et al. (1991) A gene deleted in Kallmann's syndrome shares homology with neural cell adhesion and axonal path-finding molecules. *Nature* **353**, 529–536.

Handelsman DJ, Spaliviero JA, Simpson JM, Allan CM, Singh J (1999) Spermatogenesis without gonadotrophins: maintenance has a lower testosterone threshold than initiation. *Endocrinology* **140**, 3938–3946.

Haywood M, Spaliviero J, Jimenez M, King NJ, Handelsman DJ, Allan CM (2003) Sertoli and germ cell development in hypogonadal (hpg) mice expressing transgenic follicle-stimulating hormone alone or in combination with testosterone. *Endocrinology* **144**, 509–517.

Haywood M, Tymchenko N, Spaliviero J, et al. (2002) An activated human follicle-stimulating hormone (FSH) receptor stimulates FSH-like activity in gonadotropin-deficient transgenic mice. *Mol Endocrinol* **16**, 2582–2591.

Holsberger DR, Jirawatnotai S, Kiyokawa H, Cooke PS (2003) Thyroid hormone regulates the cell cycle inhibitor p27Kip1 in postnatal murine Sertoli cells. *Endocrinology* **144**, 3732–3738.

Hosoi I, Toyama Y, Maekawa M, Ito H, Yuasa S (2002) Development of the blood–testis barrier in the mouse is delayed by neonatally administered diethylstilbestrol but not by beta-estradiol 3-benzoate. *Andrologia* **34**, 255–262.

Jackson RS, Creemers JW, Ohagi S, et al. (1997) Obesity and impaired prohormone processing associated with mutations in the human prohormone convertase 1 gene. *Nat Genet* **16**, 303–306.

Johnston H, Baker PJ, Abel M, et al. (2004) Regulation of Sertoli cell number and activity by follicle-stimulating hormone and androgen during postnatal development in the mouse. *Endocrinology* **145**, 318–329.

Kierszenbaum AI (1974) RNA synthetic activities of Sertoli cells in the mouse testis. *Biol Reprod* **11**, 365–376.

Kluin PM, Kramer MF, de Rooij DG (1984) Proliferation of spermatogonia and Sertoli cells in maturing mice. *Anat Embryol* **169**, 73–78.

Kreidberg JA, Sariola H, Loring JM, et al. (1993) WT-1 is required for early kidney development. *Cell* **74**, 679–691.

de Kretser DM, Kerr JB (1994) The cytology of the testis. In *The Physiology of Reproduction*, 2nd edn (eds Knobil E, Neill JD), pp. 1177–1290. New York: Raven Press.

Kumar TR, Varani S, Wreford NG, Telfer NM, de Kretser DM, Matzuk MM (2001) Male reproductive phenotypes in double mutant mice lacking both FSHbeta and activin receptor IIA. *Endocrinology* **142**, 3512–3518.

Luo X, Ikeda Y, Parker KL (1994) A cell-specific nuclear receptor is essential for adrenal and gonadal development and sexual differentiation. *Cell* **77**, 481–490.

Mason AJ, Hayflick JS, Zoeller RT, et al. (1986a) A deletion truncating the gonadotropin-releasing hormone gene is responsible for hypogonadism in the hpg mouse. *Science* **234**, 1366–1371.

Mason AJ, Pitts SL, Nikolics K, et al. (1986b) The hypogonadal mouse: reproductive functions restored by gene therapy. *Science* **234**, 1372–1378.

Maymon BB, Yogev L, Paz G, et al. (2002) Sertoli cell maturation in men with azoospermia of different etiologies. *Fertil Steril* **77**, 904–909.

Meachem SJ, Wreford NG, Stanton PG, Robertson DM, McLachlan RI (1998) Follicle-stimulating hormone is required for the initial phase of spermatogenic restoration in adult rats following gonadotropin suppression. *J Androl* **19**, 725–735.

Meachem SJ, McLachlan RI, Stanton PG, Robertson DM, Wreford NG (1999) FSH immunoneutralization acutely impairs spermatogonial development in normal adult rats. *J Androl* **20**, 756–762.

Millard SS, Yan JS, Nguyen H, Pagano M, Kiyokawa H, Koff A (1997) Enhanced ribosomal association of p27 (Kip1) mRNA is a mechanism contributing to accumulation during growth arrest. *J Biol Chem* **272**, 7093–7098.

Mirre C, Knibiehler B (1982) A re-evaluation of the relationships between the fibrillar centres and the nucleolus-organizing regions in reticulated nucleoli: ultrastructural organization, number and distribution of the fibrillar centres in the nucleolus of the mouse Sertoli cell. *J Cell Sci* **55**, 247–259.

Morales A, Cavicchia JC (2002) Spermatogenesis and blood–testis barrier in rats after long-term vitamin A deprivation. *Tissue Cell* **34**, 349–355.

Moroi S, Saitou M, Fujimoto K, et al. (1998) Occludin is concentrated at tight junctions of mouse/rat but not human/guinea pig Sertoli cells in testes. *Am J Physiol* **274**, C1708–C1717.

Myers M, Britt KL, Wreford NG, Ebling FJ, Kerr JB (2004) Methods for quantifying follicular numbers within the mouse ovary. *Reproduction* **127**, 569–580.

Noguchi J, Toyama Y, Yuasa S, Kikuchi K, Kaneko H (2002) Hereditary defects in both germ cells and the blood–testis barrier system in as-mutant rats: evidence from spermatogonial transplantation and tracer-permeability analysis. *Biol Reprod* **67**, 880–888.

O'Donnell L, Narula A, Balourdos G, et al. (2001) Impairment of spermatogonial development and spermiation after testosterone-induced gonadotropin suppression in adult monkeys (*Macaca fascicularis*). *J Clin Endocrinol Metab* **86**, 1814–1822.

O'Shaughnessy PJ, Sheffield JW (1990) Effect of testosterone on testicular steroidogenesis in the hypogonadal (hpg) mouse. *J Steroid Biochem* **35**, 729–734.

Oakberg EF (1956) A description of spermiogenesis in the mouse and its use in analysis of the cycle of the seminiferous epithelium and germ cell renewal. *Am J Anat* **99**, 391–414.

Pask AJ, Kanasaki H, Kaiser UB, et al. (2005) A novel mouse model of hypogonadotrophic hypogonadism: *N*-ethyl-*N*-nitrosourea-induced gonadotropin-releasing hormone receptor gene mutation. *Molec Endocrinol* **19**, 972–981.

Pelletier RM (1986) Cyclic formation and decay of the blood–testis barrier in the mink (*Mustela vison*), a seasonal breeder. *Am J Anat* **175**, 91–117.

Raleigh D, O'Donnell L, Southwick GJ, de Kretser DM, McLachlan RI (2004) Stereological analysis of the human testis after vasectomy indicates impairment of spermatogenic efficiency with increasing obstructive interval. *Fertil Steril* **81**, 1595–1603.

Robertson KM, O'Donnell L, Jones ME, et al. (1999) Impairment of spermatogenesis in mice lacking a functional aromatase (cyp 19) gene. *Proc Natl Acad Sci USA* **96**, 7986–7991.

Robertson KM, O'Donnell L, Simpson ER, Jones ME (2002) The phenotype of the aromatase knockout mouse reveals dietary phytoestrogens impact significantly on testis function. *Endocrinology* **143**, 2913–2921.

de Rooij DG, Grootegoed JA (1998) Spermatogonial stem cells. *Curr Opin Cell Biol* **10**, 694–701.

de Rooij DG, Russell LD (2000) All you wanted to know about spermatogonia but were afraid to ask. *J Androl* **21**, 776–798.

de Roux N, Genin E, Carel JC, Matsuda F, Chaussain JL, Milgrom E (2003) Hypogonadotropic hypogonadism due to loss of function of the KiSS1-derived peptide receptor GPR54. *Proc Natl Acad Sci USA* **100**, 10972–10976.

Russell LD, Bartke A, Goh JC (1989) Postnatal development of the Sertoli cell barrier, tubular lumen, and cytoskeleton of Sertoli and myoid cells in the rat, and their relationship to tubular fluid secretion and flow. *Am J Anat* **184**, 179–189.

Russell LD, Ettlin RA, SinhaHikim AP, Clegg ED (1990) *Histological and Histopathological Evaluation of the Testis*. Clearwater FL: Cache River Press.

Scott IS, Charlton HM, Cox BS, Grocock CA, Sheffield JW, O'Shaughnessy PJ (1990) Effect of LH injections on testicular steroidogenesis, cholesterol side-chain cleavage P450 mRNA content and Leydig cell morphology in hypogonadal mice. *J Endocrinol* **125**, 131–138.

Seminara SB, Messager S, Chatzidaki EE, et al. (2003) The GPR54 gene as a regulator of puberty. *N Engl J Med* **349**, 1614–1627.

Setchell BP, Zupp JP, Pollanen P (1988) Blood testis barrier at puberty. In *Development and Function of the Reproductive Organs* (eds Parvinen M, Huhtaniemi I, Pelliniemi, LJ), pp. 77–84. Rome: Serono Symp Rev.

Sharpe RM, McKinnell C, Kivlin C, Fisher JS (2003) Proliferation and functional maturation of Sertoli cells, and their relevance to disorders of testis function in adulthood. *Reproduction* **125**, 769–784.

Sheffield JW, O'Shaughnessy PJ (1988) Testicular steroid metabolism during development in the normal and hypogonadal mouse. *J Endocrinol* **119**, 257–264.

Singh J, O'Neill C, Handelsman DJ (1995) Induction of spermatogenesis by androgens in gonadotropin-deficient (hpg) mice. *Endocrinology* **136**, 5311–5321.

Singh J, Handelsman DJ (1996a) The effects of recombinant FSH on testosterone-induced spermatogenesis in gonadotrophin-deficient (hpg) mice. *J Androl* **17**, 382–393.

Singh J, Handelsman DJ (1996b) Neonatal administration of FSH increases Sertoli cell numbers and spermatogenesis in gonadotropin-deficient (hpg) mice. *J Endocrinol* **151**, 37–48.

Spaliviero JA, Jimenez M, Allan CM, Handelsman DJ (2004) Luteinizing hormone receptor-mediated effects on initiation of spermatogenesis in gonadotropin-deficient (hpg) mice are replicated by testosterone. *Biol Reprod* **70**, 32–38.

Steger K, Rey R, Louis F, et al. (1999) Reversion of the differentiated phenotype and maturation block in Sertoli cells in pathological human testis. *Human Reprod* **14**, 136–143.

Toyama Y, Maekawa M, Yuasa S (2003) Ectoplasmic specializations in the Sertoli cell: new vistas based on genetic defects and testicular toxicology. *Anat Sci Int* **78**, 1–16.

Vitale R, Fawcett DW, Dym M (1973) The normal development of the blood–testis barrier and the effects of clomiphene and estrogen treatment. *Anat Rec* **176**, 331–344.

Vogl AW, Pfeiffer DC, Redenbach DM, Grove BD (1993) Sertoli cell cytoskeleton. In *The Sertoli Cell* (eds Russell LD, Griswold MD), pp. 39–86. Clearwater FL: Cache River Press.

Wang ZQ, Todani T, Watanabe Y, et al. (1998) Germ-cell degeneration in experimental unilateral cryptorchidism: role of apoptosis. *Pediatr Surg Int* **14**, 9–13.

Wiebe JP, Kowalik A, Gallardi RL, Egeler O, Clubb BH (2000) Glycerol disrupts tight junction-associated actin microfilaments, occludin, and microtubules in Sertoli cells. *J Androl* **21**, 625–635.

Wreford NG (1995) Theory and practice of stereological techniques applied to the estimation of cell number and nuclear volume in the testis. *Microsc Res Techn* **32**, 423–436.

Wreford NG, Rajendra Kumar T, Matzuk MM, de Kretser DM (2001) Analysis of the testicular phenotype of the follicle-stimulating hormone beta-subunit knockout and the activin type II receptor knockout mice by stereological analysis. *Endocrinology* **142**, 2916–2920.

Zhengwei Y, Wreford NG, Schlatt S, Weinbauer GF, Nieschlag E, McLachlan RI (1998) Acute and specific impairment of spermatogonial development by GnRH antagonist-induced gonadotrophin withdrawal in the adult macaque (*Macaca fascicularis*). *J Reprod Fertil* **112**, 139–147.